

# A large-aperture telescope to map the CMB $10\times$ faster

MICHAEL D. NIEMACK<sup>1</sup>

<sup>1</sup>Cornell University Physics Department, Ithaca, NY 14850, USA; niemack@cornell.edu

Compiled July 18, 2022

---

Current large-aperture cosmic microwave background (CMB) telescopes have nearly maximized the number of detectors that can be illuminated while maintaining diffraction-limited image quality. The polarization-sensitive detector arrays being deployed in these telescopes in the next few years will have roughly  $10^4$  detectors. Increasing the mapping speed of future instruments by at least an order of magnitude is important to enable precise probes of the inflationary paradigm in the first fraction of a second after the big bang and provide strong constraints on cosmological parameters. This paper introduces new crossed Dragone telescope and receiver optics designs that increase the usable diffraction-limited field-of-view, and therefore the mapping speed, by over an order of magnitude to enable high efficiency illumination of  $> 10^5$  detectors in a next generation CMB telescope.

**OCIS codes:** (110.6770) Telescopes; (350.1260) Astronomical Optics; (350.4010) Microwaves; (040.1240) Detector Arrays.

<http://dx.doi.org/XXXXXX>

---

Recent measurements of the Cosmic Microwave Background (CMB) led to detections of several new cosmological signals, including gravitational lensing of the CMB, approximately mass-limited galaxy cluster catalogs, and, most recently, the “B-mode” polarization (e.g. [1–4]). This rapid progress has been enabled by the development of large arrays of background-limited low-temperature detectors. These detector arrays are typically designed to fill a large fraction of the diffraction-limited field-of-view (DLFOV) on each telescope. The upcoming generation of CMB instruments will nearly fill the DLFOV of existing large-aperture ( $> 2$  meter) telescopes with  $\mathcal{O}10^4$  detectors operating between 30 GHz – 300 GHz [5–7].

Beyond this coming generation of instruments, there is potential for substantial improvements in constraints on signals from inflationary gravity waves, neutrino properties, and other cosmological parameters if CMB measurements can be made with sufficient sensitivity and angular resolution [e.g., 8–10]. The CMB community has begun planning for a “Stage IV” CMB survey with  $\mathcal{O}10^5$  –  $10^6$  detectors to achieve these scientific goals. Since current telescopes do not have sufficient throughput to illuminate  $> 10^5$  detectors, it is important to develop designs for higher-throughput telescopes. We quantify the diffraction-limited throughput tradeoffs between crossed-Dragone telescope designs and present a design for a

crossed-Dragone telescope with close-packed reimaging optics to achieve  $\sim 10\times$  faster mapping speed than upcoming CMB surveys.

The crossed-Dragone (CD) telescope [11] has recently been recognized as an excellent choice for CMB polarimetry [for an overview, see 12] because it provides a large DLFOV with excellent polarization fidelity [13]. CD telescopes were used for CMB measurements for the first time in the last decade on two small aperture ( $< 2$  m) instruments [14, 15], and were proposed in a concept paper for NASA’s Inflation Probe[16]. All of these designs have small focal ratios ( $f < 2$ ) and place the detector arrays directly at the telescope focus. This presents a challenging baffling problem due to substantial spillover past both the primary and secondary mirrors, which has been mitigated by use of absorbing baffles. In the Atacama B-mode Search [15] the telescope mirrors and baffles are cooled to  $\sim 4$  K temperatures to minimize loading and photon noise from the baffles. In the Q/U Imaging Experiment [14] coherent detectors are used to directly measure the polarization signal, thereby reducing sensitivity to unpolarized emission from the ambient temperature baffles.

Here we present CD telescope designs with larger apertures ( $> 2$  m) and focal ratios ( $2 < f < 3$ ) that mitigate the CD baffling challenges by coupling to reimaging optics with a cryogenic Lyot stop at an image of the primary

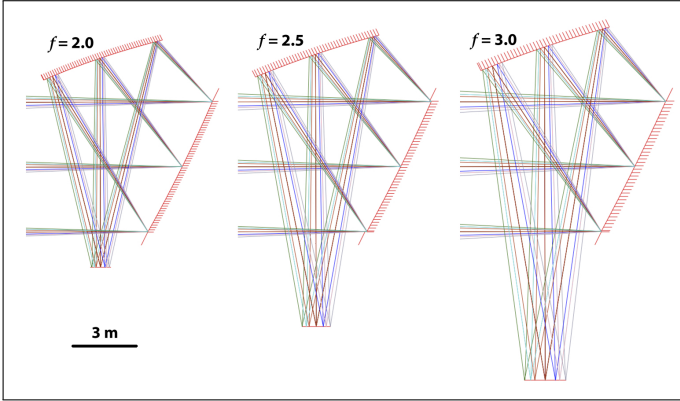


**Fig. 1.** Three 6 m aperture telescope designs with different  $f$ . Plotted rays span the 150 GHz CFOV with Strehl ratios  $> 0.70$ .

mirror. Similar Lyot stops are used in both current [3, 17] and upcoming [5–7] large-aperture CMB instruments, because they can suppress spillover outside the main beam by over an order of magnitude and dramatically reduce baffling requirements. Fig. 1 shows three example CD designs with different  $f$ , and Fig. 2 depicts the substantial increase in DLFOV as the  $f$  and aperture are increased. The implementation of these designs follows [18] in which the following five parameters are chosen to define the design: the primary diameter,  $D_m$ , the angle between the mirror and focal plane coordinate systems,  $\theta_p$ , the primary mirror focal length,  $F$ , the distance between the secondary mirror and focal plane,  $L_s$ , and the half angle between the focal plane and secondary mirror,  $\theta_e$ , which defines the focal ratio,  $f = [2 \tan(\theta_e)]^{-1}$ . Tab. 1 provides design parameters for the telescopes in Fig. 1 and 3. In practice, these parameters are implemented in ray tracing software, then the distances between primary and secondary as well as secondary and focal plane are optimized to improve the image quality across a wide FOV.

The DLFOV for each telescope design is calculated by adjusting the major and minor axis of an elliptical FOV until the 150 GHz Strehl ratios of the extreme  $\pm X$  and  $\pm Y$  fields are  $0.80 \pm 0.01$ , which is commonly regarded as the minimum “diffraction-limited” Strehl ratio. The throughput is then calculated as the area times the solid angle at both the telescope aperture and focal plane for consistency. A similar approach is used to calculate the throughput for different wavelengths (100 GHz, 230 GHz, and 300 GHz) and minimum Strehl ratios (0.70 and 0.90) shown in Fig. 2 and 4. As described below, we find that reimaging optics can be used to correct local aberrations, and thereby improve the minimum Strehl ratios in each field from 0.70 to  $> 0.80$ . We therefore define the “correctable” field-of-view (CFOV) as the field-of-view with Strehl ratios  $> 0.70$ .

In Fig. 2 we also compare the throughput of CD telescopes to the 6 m off-axis, numerically-optimized, aplanatic Gregorian design used for the Atacama Cosmology

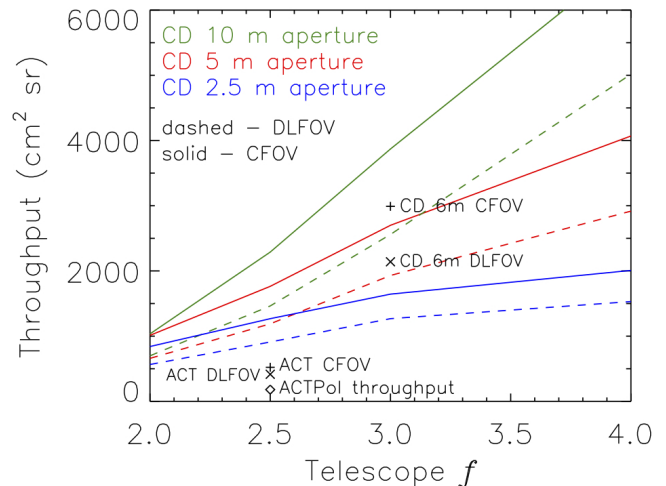


**Fig. 2.** Telescope  $f$  versus throughput for different telescope apertures (2.5 m - blue/lowest, 5 m - red, 10 m - green/highest). Solid (dashed) lines indicate the telescope 150 GHz CFOV (DLFOV). Also shown are points indicating the 150 GHz throughput of the ACT FOVs, ACTPol, and the CD 6 m design in Fig. 3 and 4.

Telescope (ACT, [19]).<sup>1</sup> We find that CD designs have substantially larger DLFOV and CFOV than the ACT; specifically, the 6 m  $f = 3$  design in Fig. 3 has  $> 5\times$  larger DLFOV than the ACT and the receiver optics presented here have  $> 10\times$  larger throughput than the ACTPol [17] throughput shown in Fig. 2.

We highlight a 6 m telescope design that combines sufficiently large throughput to achieve  $> 10\times$  faster mapping speed than upcoming instruments with sufficient resolution to pursue the full range CMB survey science, from inflation to galaxy clusters. Fig. 3 shows an  $f = 3$  telescope design in which a flat tertiary mirror has been added to fold the optics and make the design more compact. This moves the receiver closer to the axis of rotation of the telescope when observing at a nominal elevation of  $45^\circ$ . The  $f = 3$  designs in Fig. 1 and 3 have different spacings between the primary, secondary, tertiary, and receiver, which can be easily adjusted to provide space for baffling without significant changes in throughput, as indicated in Tab. 1. Unlike traditional Gregorian telescopes, these CD designs may be sufficiently compact to enable boresight rotations of the entire telescope around the optical axis to mitigate optical systematics that could lead to spurious polarization signals.

Over the last decade several teams have studied and implemented reimaging optics designs for large-aperture CMB telescopes and have converged on using optics tubes with multiple lenses. The upcoming instruments for the ACT [7], SPT [6], and Simons Array [5] will all employ an optics-tube approach in which three lenses reimaging the telescope focus onto each detector array. The detector arrays on these instruments will be superconducting bolo-

<sup>1</sup>See [12] for a comparison of the ACT and South Pole Telescope [20] optics.

metric detectors operated at sub-Kelvin temperatures that are sensitive to excess thermal emission. These detectors are generally optimized to achieve “background-limited” sensitivity, meaning that photon noise fluctuations are the dominant noise source. When detectors are “background-limited” the best approaches for improving sensitivity are generally to reduce the backgrounds and increase the number of detectors while maintaining the throughput per detector.

Coupling the detectors to a CD telescope via multiple optics tubes amplifies the CD benefits in several ways, including: 1) increasing the usable FOV diameter, 2) providing a compact cryogenic Lyot stop that mitigates spillover, simplifies baffling, and increases sensitivity by reducing the background optical load, 3) dividing a large cryostat window into smaller ones, which reduces window and lens size, thickness, and coating complexity, and 4) maximizing the number of detectors in each silicon wafer to reduce costs and increase sensitivity. The cryogenic Lyot stop also provides uniform illumination for half-wave-plate polarization modulators to mitigate systematic effects.

The detector arrays illuminated by these optics can generally be described as “feed-coupled” detectors with single-moded approximately Gaussian beams. The “feed” may be a feedhorn, a lenslet, or a phased-antenna array [e.g., 12]. The Gaussian optics are typically designed such that a substantial fraction of the beam (10 – 50%) illuminates the Lyot stop, baffles, and walls surrounding the detector array. This highlights the importance of reducing the temperature of these baffles, which even at 4 K could contribute more optical loading and photon noise than the 2.7 K CMB. In [21] the tradeoffs between detector aperture and background loading levels are explored for a variety of different configurations. For close-packed “feed-coupled” arrays after minimizing sources of background loading, the optimal detector aperture for measuring an extended source like the CMB is generally between  $1 - 2 f\lambda$ , where  $\lambda$  is the wavelength, which is the regime of most current detector arrays. For FOV-limited designs with no limit on the detector packing density, the optimal spacing when taking into account instrument backgrounds is typically near  $1.3 - 1.5 f\lambda$ , while readout-limited or detector-packing-limited arrays are typically

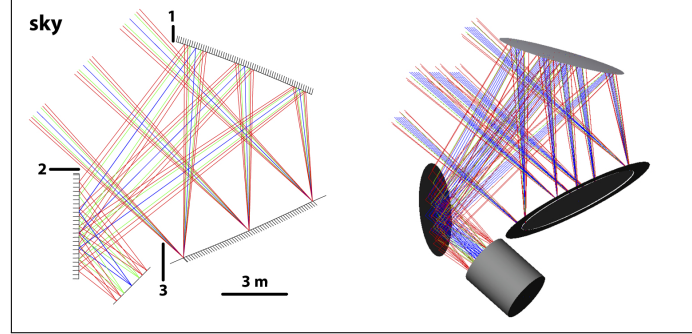


**Fig. 3.** A 6 m aperture CD telescope design tilted to a  $45^\circ$  observing elevation with  $f = 3$  and a flat tertiary mirror to move the telescope focus and receiver closer to the center of mass. The rendered image on the right also shows a cylindrical receiver for the optics tubes. Note that the optical clearances labeled 1, 2, and 3 can easily be adjusted by changing the telescope parameters (Tab. 1).

designed with apertures closer to  $2 f\lambda$ .

The first multi-frequency, or multichroic, detector array was deployed in early 2015 [7], and more will be deployed soon in upcoming CMB instruments [5–7]. These arrays enable use of greater bandwidth and simultaneous observations at multiple frequency bands at the cost of building and reading out more detectors from each focal plane element. Additional challenges include that each frequency is typically coupled through the same “feed”, which leads to tradeoffs between the optimal aperture size at each frequency. For example, [22] presents an analysis of optimal aperture size to maximize the mapping speed at different frequencies for the ACTPol design [17], which has  $f \approx 1.35$  and a 1 K detector cavity extending to the Lyot stop. This analysis suggests the optimal apertures for 90 GHz, 150 GHz, and 220 GHz are between 1.3–1.4  $f\lambda$ , which corresponds to approximately 6 mm, 3.7 mm, and 2.4 mm feed apertures, respectively.<sup>2</sup> Clearly the optimal aperture cannot be achieved for all three frequencies simultaneously. A two frequency multichroic array can achieve the mapping speed of  $\sim 1.7$  optimized single frequency arrays in addition to improved spectral coverage [22]. This and the challenges of developing wide bandwidth optics to couple to multichroic arrays suggests a reasonable number of frequencies for a “feed-coupled” multichroic array is two or three.

The multichroic detector arrays for upcoming large-aperture CMB instruments are all expected to be fabricated on 150 mm diameter silicon wafers.<sup>3</sup> Superconducting detector fabrication is challenging and costly due to detector complexity and strict uniformity requirements [e.g., 7]; therefore, it is generally advantageous to make each wafer as sensitive as possible by maximizing the number

<sup>2</sup>The optimal apertures for ACTPol assume a fixed field-of-view and no constraint on the number of detectors per array.

<sup>3</sup>Previously deployed detectors were fabricated on 75 mm or 100 mm wafers.

**Table 1.** Variable telescope parameters for Fig. 1 and 3. Constant parameters are  $D_m = 6.0$  m and  $\theta_p = 90^\circ$  as defined in [18]. Throughput,  $A\Omega$ , is given for the 150 GHz CFOV.

Figure, $f$	$F$ (m)	$\theta_e$ ( $^\circ$ )	$L_s$ (m)	$A\Omega$ ( $\text{cm}^2 \text{ sr}$ )
1, 2.0	24.1	14.05	8.8	1010
1, 2.5	30.0	11.3	11.5	1950
1, 3.0	36.0	9.45	14.0	2990
3, 3.0	30.0	9.45	18.6	3000

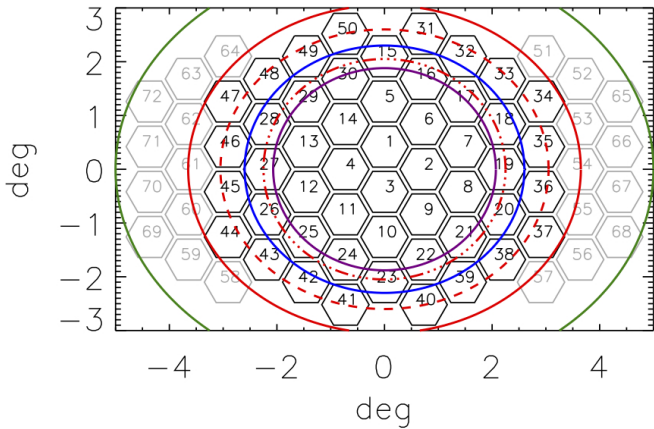


**Fig. 4.** Telescope FOV for the design in Fig. 3. The solid ellipses show the CFOV for 300 GHz (inner/purple), 230 GHz (blue), 150 GHz (red), and 100 GHz (outer/green). The red dash and dot-dash ellipses show the FOV with 150 GHz Strehl ratios  $> 0.80$  and  $> 0.90$ , respectively. The black hexagons indicate a possible layout for 50 optics tubes that can achieve diffraction-limited performance at 150 GHz. The additional 22 grey hexagons on the left and right indicate possible locations for additional optics tubes that would be diffraction-limited at 100 GHz and at lower foreground frequencies, such as 30 GHz and 40 GHz. Each hexagon represents a 280 mm diameter hexagonal shaped lens with 25 mm gaps between lenses. The plate scale is approximately 320 mm/deg.

of detectors per wafer, so long as the additional detectors do not complicate fabrication. All of the upcoming large-aperture projects plan to use hex-packed detectors on hexagonal-shaped detector wafers surrounded by wirebond pads to read out the detectors. In Advanced ACTpol the densest of these arrays will have 2012 superconducting detectors operating at 150 GHz and 230 GHz with 4.65 mm apertures [7]. For SPT-3G each detector wafer will have a slightly smaller number of detectors operating at 95 GHz, 150 GHz, and 220 GHz, though a larger total number of detectors will be integrated into the focal plane from  $\sim 10$  wafers [6]. These designs are approaching the practical limits of both wirebond density and detector-packing density, though a factor of  $\sim 1.5$  increase in detector count per 150 mm wafer may be achieved for a Stage IV experiment. For the purpose of this study, we assume that next generation detectors will have 2000 – 3000 detectors per 150 mm wafer.

These considerations guide the design of the reimaging optics. Around the perimeter of each hexagonal detector wafer there is inevitably some dead space (e.g. bond pads and mechanical structure) that does not couple light to detectors. This dead space decreases the effective system throughput. By designing hex-packed optics tubes that each couple to a single detector wafer, we remove the dead space from around the detector arrays and provide more space for support structures, while introducing a

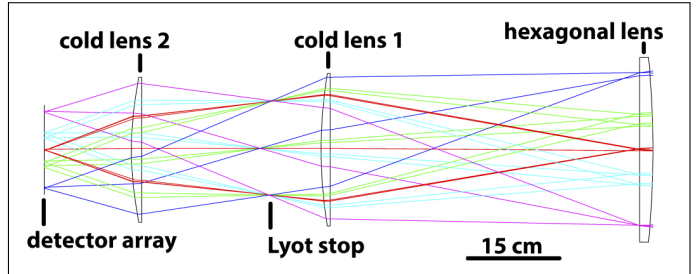


**Fig. 5.** Reimaging optics that speed up the telescope focus from  $f = 3$  to  $f = 1.5$  and provide a Lyot stop to control primary mirror illumination and spillover. The hexagonal lens is at the telescope focus and could also be used as a room-temperature vacuum window. The two cryogenic lenses are circular and fit inside the footprint of the hexagonal lens to facilitate thermal isolation between temperature stages.

small amount of dead space into the telescope focal plane. To minimize the dead space between optics tubes, the first modular element in each tube is a hexagonal refractive lens that captures and collimates the telescope beam before it diverges beyond the telescope focus. Based on the design in Fig. 3, we divide the CFOV into 50 hexagonal fields, each with a maximum dimension of 280 mm and a 25 mm space for structural support between neighboring lenses (Fig. 4). This geometry provides roughly 90% active area with greater throughput than the 150 GHz DLFOV, which is  $> 10 \times$  the ACTPol throughput (Fig. 4).

After the hexagonal lens, each subsequent optical aperture and cryogenic support structure should fit inside the footprint of the first lens to prevent interference between optics tubes. One cryogenic lens helps to optimize the Lyot stop and image quality, and a final lens improves the image quality and telecentricity, while focusing at  $f = 1.5$  onto the 140 mm wide active area of a hexagonal detector array. The second and third lenses are not at a focus, so they have circular instead of hexagonal apertures, and therefore must be smaller diameter than the smallest dimension of the hexagonal lens (242 mm). The design shown in Fig. 5 meets these requirements and uses silicon lenses [23]<sup>4</sup> to improve on the local image quality at the telescope focus. Nearly identical optics tube designs have been shown to achieve Strehl ratios  $> 0.80$  at 150 GHz for all of optics tubes 1 – 50 in Fig. 4.

A different receiver optics approach based on larger-diameter (720 mm) alumina lenses is being pursued for the SPT-3G instrument [6]. This approach is appealing from the optics design perspective and appropriate for current instruments; however, it presents challenges for next generation instruments that can be avoided by use of close-packed optics tubes. Larger-diameter lenses are necessarily thicker at the center, which results in greater loss within each refractive element. Having a single optics tube also requires development of wider-bandwidth high-

<sup>4</sup>Similar optical performance is likely achievable with alumina lenses.

efficiency coatings for all optical elements. In comparison, the optics tubes in Fig. 4 can easily be divided for use over a wide frequency range; for example, tubes 1–14 could be used with multichroic 220/300 GHz arrays (or lower frequencies), tubes 15–50 with 100/150 GHz arrays, and tubes 51–72 with 30/40 GHz (or up to 100 GHz) arrays. Implementing six or more frequency bands spanning 30–300 GHz on a single telescope would be far more difficult with a single set of large diameter lenses.

With the close-packed optics tube approach described here, if detector array designs for upcoming instruments with  $\sim$ 2000 detectors per wafer were installed into optics tubes 1–50 in Fig. 4, that would provide  $\mathcal{O}10^5$  detectors on one telescope. However, with  $f = 1.5$  at the optics tube focus, the mapping speed could be increased further by modestly increasing the number of detectors on each wafer. For example, if either a third frequency were added to the Advanced ACTPol detector arrays or the feed aperture for the multichroic 150/230 GHz detectors was decreased from 4.65 mm to 3.9 mm (resulting in  $\sim 1.3 f\lambda$  at 150 GHz and  $\sim 2 f\lambda$  at 230 GHz), it could provide roughly 3000 detectors per wafer with a good balance of aperture efficiencies. In this case, or by including optics tubes 51–72 in Fig. 4 at lower frequencies, the optics design presented here could illuminate  $>150,000$  diffraction-limited superconducting detectors.

We have shown that one large-aperture CMB telescope can illuminate  $>10\times$  more detectors between 30–300 GHz and provide approximately  $10\times$  faster mapping speed than upcoming CMB instruments. Our approach is based on a crossed-Dragone telescope design with modular close-packed optics tubes filling the telescope focal plane. This demonstrates that a Stage IV CMB observatory with  $\mathcal{O}10^5$ – $10^6$  detectors can be built using a small number of telescopes.

## FUNDING INFORMATION:

National Science Foundation CAREER award number 1454881.

## ACKNOWLEDGMENTS

The author thanks L. A. Page, A. T. Lee, S. T. Staggs, S. Dicker, G. Stacey, N. W. Halverson, J. J. McMahon, M. J. Devlin, S. Padin, J. E. Carlstrom, J. W. Fowler, S. Hanany, S. W. Henderson, B. J. Koopman, S. M. Bruno, and attendees of the 2015 CMB-S4 meeting for useful discussions and/or comments.

## REFERENCES

- D. Hanson, S. Hoover, A. Crites, P. A. R. Ade, K. A. Aird, J. E. Austermann, J. A. Beall, A. N. Bender, B. A. Benson, L. E. Bleem, J. J. Bock, J. E. Carlstrom, C. L. Chang, H. C. Chiang, H.-M. Cho, A. Conley, T. M. Crawford, T. de Haan, M. A. Dobbs, W. Everett, J. Gallicchio, J. Gao, E. M. George, N. W. Halverson, N. Harrington, J. W. Henning, G. C. Hilton, G. P. Holder, W. L. Holzapfel, J. D. Hrubes, N. Huang, J. Hubmayr, K. D. Irwin, R. Keisler, L. Knox, A. T. Lee, E. Leitch, D. Li, C. Liang, D. Luong-Van, G. Marsden, J. J. McMahon, J. Mehl, S. S. Meyer, L. Mocanu, T. E. Montroy, T. Natoli, J. P. Nibarger, V. Novosad, S. Padin, C. Pryke, C. L. Reichardt, J. E. Ruhl, B. R. Saliwanchik, J. T. Sayre, K. K. Schaffer, B. Schulz, G. Smecher, A. A. Stark, K. T. Story, C. Tucker, K. Vanderlinde, J. D. Vieira, M. P. Viero, G. Wang, V. Yefremenko, O. Zahn, and M. Zemcov, "Detection of B-Mode Polarization in the Cosmic Microwave Background with Data from the South Pole Telescope," *Physical Review Letters* **111**, 141301 (2013).
- BICEP2/Keck and Planck Collaborations, P. A. R. Ade, N. Aghanim, Z. Ahmed, R. W. Aikin, K. D. Alexander, M. Arnaud, J. Aumont, C. Bacigalupi, A. J. Banday, D. Barkats, R. B. Barreiro, J. G. Bartlett, N. Bartolo, E. Battaner, K. Benabed, A. Benoît, A. Benoit-Lévy, S. J. Benton, J. P. Bernard, M. Bersanelli, P. Bielewicz, C. A. Bischoff, J. J. Bock, A. Bonaldi, L. Bonavera, J. R. Bond, J. Borrill, F. R. Bouchet, F. Boulanger, J. A. Brevik, M. Bucher, I. Buder, E. Bullock, C. Burigana, R. C. Butler, V. Buza, E. Calabrese, J. F. Cardoso, A. Catalano, A. Challinor, R. R. Chary, H. C. Chiang, P. R. Christensen, L. P. L. Colombo, C. Combet, J. Connors, F. Couchot, A. Coulais, B. P. Crill, A. Curto, F. Cuttaia, L. Danese, R. D. Davies, R. J. Davis, P. de Bernardis, A. De Rosa, G. de Zotti, J. Delabrouille, J. M. Delouis, F. X. Désert, C. Dickinson, J. M. Diego, H. Dole, S. Donzelli, O. Doré, M. Douspis, C. D. Dowell, L. Duband, A. Ducout, J. Dunkley, X. Dupac, C. Dvorkin, G. Efstathiou, F. Elsner, T. A. Enßlin, H. K. Eriksen, E. Falgarone, J. P. Filippini, F. Finelli, S. Fliescher, O. Forni, M. Frailis, A. A. Fraisse, E. Franceschi, A. Frejsel, S. Galeotta, S. Galli, K. Ganga, T. Ghosh, M. Giard, E. Gjerløw, S. R. Golwala, J. González-Nuevo, K. M. Górski, S. Gratton, A. Gregorio, A. Gruppuso, J. E. Gudmundsson, M. Halpern, F. K. Hansen, D. Hanson, D. L. Harrison, M. Hasselfield, G. Helou, S. Henrot-Versillé, D. Herranz, S. R. Hildebrandt, G. C. Hilton, E. Hivon, M. Hobson, W. A. Holmes, W. Hovest, V. V. Hristov, K. M. Huffenberger, H. Hui, G. Hurier, K. D. Irwin, A. H. Jaffe, T. R. Jaffe, J. Jewell, W. C. Jones, M. Juvela, A. Karakci, K. S. Karkare, J. P. Kaufman, B. G. Keating, S. Kefeli, E. Keihänen, S. A. Kernasovskiy, R. Keskitalo, T. S. Kisner, R. Kneissl, J. Knoche, L. Knox, J. M. Kovac, N. Krachmalnicoff, M. Kunz, C. L. Kuo, H. Kurki-Suonio, G. Lagache, A. Lähteenmäki, J. M. Lamarre, A. Lasenby, M. Lattanzi, C. R. Lawrence, E. M. Leitch, R. Leonardi, F. Levrier, A. Lewis, M. Liguori, P. B. Lilje, M. Linden-Vørnle, M. López-Caniego, P. M. Lubin, M. Lueker, J. F. Macías-Pérez, B. Maffei, D. Maino, N. Mandolesi, A. Mangilli, M. Maris, P. G. Martin, E. Martínez-González, S. Masi, P. Mason, S. Matarrese, K. G. Megerian, P. R. Meinhold, A. Melchiorri, L. Mendes, A. Mennella, M. Migliaccio, S. Mitra, M. A. Miville-Deschénes, A. Moneti, L. Montier, G. Morgante, D. Mortlock, A. Moss, D. Munshi, J. A. Murphy, P. Naselsky, F. Nati, P. Natoli, C. B. Netterfield, H. T. Nguyen, H. U. Nørgaard-Nielsen, F. Noviello, D. Novikov, I. Novikov, R. O'Brient, R. W. Ogburn, A. Orlando, L. Pagano, F. Pajot, R. Paladini, D. Paoletti, B. Partridge, F. Pasian, G. Patanchon, T. J. Pearson, O. Perdereau, L. Perotto, V. Pettorino, F. Piacentini, M. Piat, D. Pietrobon, S. Plaszczynski, E. Pointecouteau, G. Polenta, N. Ponthieu, G. W. Pratt, S. Prunet, C. Pryke, J. L. Puget, J. P. Rachen, W. T. Reach, R. Rebolo, M. Reinecke, M. Remazeilles, C. Renault, A. Renzi, S. Richter, I. Ristorcelli, G. Rocha, M. Rossetti, G. Roudier, M. Rowan-Robinson, J. A. Rubiño Martín, B. Rusholme, M. Sandri, D. Santos, M. Savelainen, G. Savini, R. Schwarz, D. Scott, M. D. Seiffert, C. D. Sheehy, L. D. Spencer, Z. K. Staniszewski, V. Stolyarov, R. Sudiwala, R. Sunyaev, D. Sutton, A. S. Suur-Uiski, J. F. Sygnet, J. A. Tauber, G. P. Teply, L. Terenzi, K. L. Thompson, L. Toffolatti, J. E. Tolan, M. Tomasi, M. Tristram, M. Tucci, A. D. Turner, L. Valenziano, J. Valiviita, B. van Tent, L. Vibert, P. Vielva, A. G. Vieregg, F. Villa, L. A. Wade, B. D. Wandelt, R. Watson, A. C. Weber, I. K. Wehus, M. White, S. D. M. White, J. Willmert, C. L. Wong, K. W. Yoon, D. Yvon, A. Zacchei, and A. Zonca, "Joint Analysis of BICEP2/Keck Array and Planck Data," *Physical Review Letters* **114**, 101301 (2015).
- P. A. R. Ade, Y. Akiba, A. E. Anthony, K. Arnold, M. Atlas, D. Barron, D. Boettger, J. Borrill, S. Chapman, Y. Chinone, M. Dobbs, T. Ellefson, J. Errard, G. Fabbian, C. Feng, D. Flanigan, A. Gilbert, W. Grainger, N. W. Halverson, M. Hasegawa, K. Hattori, M. Hazumi, W. L. Holzapfel, Y. Hori, J. Howard, P. Hyland, Y. Inoue, G. C. Jaehnig, A. Jaffe, B. Keating, Z. Kermish, R. Keskitalo, T. Kisner, M. Le Jeune, A. T. Lee, E. Lin-

- der, E. M. Leitch, M. Lungu, F. Matsuda, T. Matsumura, X. Meng, N. J. Miller, H. Morii, S. Moyerman, M. J. Myers, M. Navaroli, H. Nishino, H. Paar, J. Peloton, E. Quealy, G. Rebeiz, C. L. Reichardt, P. L. Richards, C. Ross, I. Schanning, D. E. Schenck, B. Sherwin, A. Shimizu, C. Shimmin, M. Shimon, P. Sirianasak, G. Smecher, H. Spieler, N. Stebor, B. Steinbach, R. Stompor, A. Suzuki, S. Takakura, T. Tomaru, B. Wilson, A. Yadav, O. Zahn, and Polarbear Collaboration, "Measurement of the Cosmic Microwave Background Polarization Power Spectrum with the POLARBEAR Experiment," *Physical Review Letters* **113**, 021301 (2014).
4. A. van Engelen, B. D. Sherwin, N. Sehgal, G. E. Addison, R. Allison, N. Battaglia, F. de Bernardis, J. R. Bond, E. Calabrese, K. Coughlin, D. Crichton, R. Datta, M. J. Devlin, J. Dunkley, R. Dünner, P. Gallardo, E. Grace, M. Gralla, A. Hajian, M. Hasselfield, S. Henderson, J. C. Hill, M. Hilton, A. D. Hincks, R. Hlozek, K. M. Huffenberger, J. P. Hughes, B. Koopman, A. Kosowsky, T. Louis, M. Lungu, M. Madhavacheril, L. Maurin, J. McMahon, K. Moodley, C. Munson, S. Naess, F. Nati, L. Newburgh, M. D. Niemack, M. R. Nolta, L. A. Page, C. Pappas, B. Partridge, B. L. Schmitt, J. L. Sievers, S. Simon, D. N. Spergel, S. T. Staggs, E. R. Switzer, J. T. Ward, and E. J. Wollack, "The Atacama Cosmology Telescope: Lensing of CMB Temperature and Polarization Derived from Cosmic Infrared Background Cross-correlation," *Astrophysical Journal* **808**, 7 (2015).
  5. K. Arnold, N. Stebor, P. A. R. Ade, Y. Akiba, A. E. Anthony, M. Atlas, D. Barron, A. Bender, D. Boettger, J. Borrill, S. Chapman, Y. Chinone, A. Cukierman, M. Dobbs, T. Ellefot, J. Errard, G. Fabbian, C. Feng, A. Gilbert, N. Goeckner-Wald, N. W. Halverson, M. Hasegawa, K. Hattori, M. Hazumi, W. L. Holzapfel, Y. Hori, Y. Inoue, G. C. Jaehnig, A. H. Jaffe, N. Katayama, B. Keating, Z. Kermish, R. Keskitalo, T. Kisner, M. Le Jeune, A. T. Lee, E. M. Leitch, E. Linder, F. Matsuda, T. Matsumura, X. Meng, N. J. Miller, H. Morii, M. J. Myers, M. Navaroli, H. Nishino, T. Okamura, H. Paar, J. Peloton, D. Poletti, C. Raum, G. Rebeiz, C. L. Reichardt, P. L. Richards, C. Ross, K. M. Rotermann, D. E. Schenck, B. D. Sherwin, I. Shirley, M. Sholl, P. Sirianasak, G. Smecher, B. Steinbach, R. Stompor, A. Suzuki, J. Suzuki, S. Takada, S. Takakura, T. Tomaru, B. Wilson, A. Yadav, and O. Zahn, "The Simons Array: expanding POLARBEAR to three multi-chroic telescopes," *Society of Photo-Optical Instrumentation Engineers (SPIE) Conference Series* **9153**, 91531F (2014).
  6. B. A. Benson, P. A. R. Ade, Z. Ahmed, S. W. Allen, K. Arnold, J. E. Austermann, A. N. Bender, L. E. Bleem, J. E. Carlstrom, C. L. Chang, H. M. Cho, J. F. Cliche, T. M. Crawford, A. Cukierman, T. de Haan, M. A. Dobbs, D. Dutcher, W. Everett, A. Gilbert, N. W. Halverson, D. Hanson, N. L. Harrington, K. Hattori, J. W. Henning, G. C. Hilton, G. P. Holder, W. L. Holzapfel, K. D. Irwin, R. Keisler, L. Knox, D. Kubik, C. L. Kuo, A. T. Lee, E. M. Leitch, D. Li, M. McDonald, S. S. Meyer, J. Montgomery, M. Myers, T. Natoli, H. Nguyen, V. Novosad, S. Padin, Z. Pan, J. Pearson, C. Reichardt, J. E. Ruhl, B. R. Saliwanchik, G. Simard, G. Smecher, J. T. Sayre, E. Shirokoff, A. A. Stark, K. Story, A. Suzuki, K. L. Thompson, C. Tucker, K. Vanderlinde, J. D. Vieira, A. Vikhlinin, G. Wang, V. Yefremenko, and K. W. Yoon, "SPT-3G: a next-generation cosmic microwave background polarization experiment on the South Pole telescope," *Society of Photo-Optical Instrumentation Engineers (SPIE) Conference Series* **9153**, 91531P (2014).
  7. S. W. Henderson, R. Allison, J. Austermann, T. Baildon, N. Battaglia, J. A. Beall, D. Becker, F. De Bernardis, J. R. Bond, E. Calabrese, S. K. Choi, K. P. Coughlin, K. T. Crowley, R. Datta, M. J. Devlin, S. M. Duff, R. Dunner, J. Dunkley, A. van Engelen, P. A. Gallardo, E. Grace, M. Hasselfield, F. Hills, G. C. Hilton, A. D. Hincks, R. Hlozek, S. P. Ho, J. Hubmayr, K. Huffenberger, J. P. Hughes, K. D. Irwin, B. J. Koopman, A. B. Kosowsky, D. Li, J. McMahon, C. Munson, F. Nati, L. Newburgh, M. D. Niemack, P. Niraula, L. A. Page, C. G. Pappas, M. Salatino, A. Schillaci, B. L. Schmitt, N. Sehgal, B. D. Sherwin, J. L. Sievers, S. M. Simon, D. N. Spergel, S. T. Staggs, J. R. Stevens, R. Thornton, J. Van Lanen, E. M. Vavagiakis, J. T. Ward, and E. J. Wollack, "Advanced ACTPol Cryogenic Detector Arrays and Readout," *arXiv*, 1510.02809 (2015).
  8. K. N. Abazajian, K. Arnold, J. Austermann, B. A. Benson, C. Bischoff, J. Bock, J. R. Bond, J. Borrill, I. Buder, D. L. Burke, E. Calabrese, J. E. Carlstrom, C. S. Carvalho, C. L. Chang, H. C. Chiang, S. Church, A. Cooray, T. M. Crawford, B. P. Crill, K. S. Dawson, S. Das, M. J. Devlin, M. Dobbs, S. Dodelson, O. Doré, J. Dunkley, J. L. Feng, A. Fraisse, J. Gallicchio, S. B. Giddings, D. Green, N. W. Halverson, S. Hanany, D. Hanson, S. R. Hildebrandt, A. Hincks, R. Hlozek, G. Holder, W. L. Holzapfel, K. Honscheid, G. Horowitz, W. Hu, J. Hubmayr, K. Irwin, M. Jackson, W. C. Jones, R. Kalosh, M. Kamionkowski, B. Keating, R. Keisler, W. Kinney, L. Knox, E. Komatsu, J. Kovac, C.-L. Kuo, A. Kusaka, C. Lawrence, A. T. Lee, E. Leitch, A. Linde, E. Linder, P. Lubin, J. Maldacena, E. Martinec, J. McMahon, A. Miller, V. Mukhanov, L. Newburgh, M. D. Niemack, H. Nguyen, H. T. Nguyen, L. Page, C. Pryke, C. L. Reichardt, J. E. Ruhl, N. Sehgal, U. Seljak, L. Senatore, J. Sievers, E. Silverstein, A. Slosar, K. M. Smith, D. Spergel, S. T. Staggs, A. Stark, R. Stompor, A. G. Vieregg, G. Wang, S. Watson, E. J. Wollack, W. L. K. Wu, K. W. Yoon, O. Zahn, and M. Zaldarriaga, "Inflation physics from the cosmic microwave background and large scale structure," *Astroparticle Physics* **63**, 55–65 (2015).
  9. K. N. Abazajian, K. Arnold, J. Austermann, B. A. Benson, C. Bischoff, J. Bock, J. R. Bond, J. Borrill, E. Calabrese, J. E. Carlstrom, C. S. Carvalho, C. L. Chang, H. C. Chiang, S. Church, A. Cooray, T. M. Crawford, K. S. Dawson, S. Das, M. J. Devlin, M. Dobbs, S. Dodelson, O. Doré, J. Dunkley, J. Errard, A. Fraisse, J. Gallicchio, N. W. Halverson, S. Hanany, S. R. Hildebrandt, A. Hincks, R. Hlozek, G. Holder, W. L. Holzapfel, K. Honscheid, W. Hu, J. Hubmayr, K. Irwin, W. C. Jones, M. Kamionkowski, B. Keating, R. Keisler, L. Knox, E. Komatsu, J. Kovac, C.-L. Kuo, C. Lawrence, A. T. Lee, E. Leitch, E. Linder, P. Lubin, J. McMahon, A. Miller, L. Newburgh, M. D. Niemack, H. Nguyen, H. T. Nguyen, L. Page, C. Pryke, C. L. Reichardt, J. E. Ruhl, N. Sehgal, U. Seljak, J. Sievers, E. Silverstein, A. Slosar, K. M. Smith, D. Spergel, S. T. Staggs, A. Stark, R. Stompor, A. G. Vieregg, G. Wang, S. Watson, E. J. Wollack, W. L. K. Wu, K. W. Yoon, and O. Zahn, "Neutrino physics from the cosmic microwave background and large scale structure," *Astroparticle Physics* **63**, 66–80 (2015).
  10. E.-M. Mueller, F. de Bernardis, R. Bean, and M. D. Niemack, "Constraints on Gravity and Dark Energy from the Pairwise Kinematic Sunyaev-Zel'dovich Effect," *Astrophysical Journal* **808**, 47 (2015).
  11. C. Dragone, "Offset multireflector antennas with perfect pattern symmetry and polarization discrimination," *AT&T Technical Journal* **57**, 2663–2684 (1978).
  12. S. Hanany, M. D. Niemack, and L. Page, *CMB Telescopes and Optical Systems* (Springer, 2013), p. 431.
  13. Y. Mizugutchi, M. Akagawa, and H. Yokoi, "Offset Dual Reflector Antenna," *ISA Proceedings* pp. 2–5 (1976).
  14. C. Bischoff, A. Brizius, I. Buder, Y. Chinone, K. Cleary, R. N. Dumoulin, A. Kusaka, R. Monsalve, S. K. Næss, L. B. Newburgh, G. Nixon, R. Reeves, K. M. Smith, K. Vanderlinde, I. K. Wehus, M. Bogdan, R. Bustos, S. E. Church, R. Davis, C. Dickinson, H. K. Eriksen, T. Gaier, J. O. Gundersen, M. Hasegawa, M. Hazumi, C. Holler, K. M. Huffenberger, W. A. Imbriale, K. Ishidohiro, M. E. Jones, P. Kangaslahti, D. J. Kapner, C. R. Lawrence, E. M. Leitch, M. Limon, J. J. McMahon, A. D. Miller, M. Nagai, H. Nguyen, T. J. Pearson, L. Piccirillo, S. J. E. Radford, A. C. S. Readhead, J. L. Richards, D. Samtleben, M. Seiffert, M. C. Shepherd, S. T. Staggs, O. Tajima, K. L. Thompson, R. Williamson, B. Winstein, E. J. Wollack, and J. T. L. Zwart, "The Q/U Imaging ExperimentT Instrument," *Astrophysical Journal* **768**, 9 (2013).
  15. T. Essinger-Hileman, J. W. Appel, J. A. Beal, H. M. Cho, J. Fowler, M. Halpern, M. Hasselfield, K. D. Irwin, T. A. Marriage, M. D. Niemack, L. Page, L. P. Parker, S. Pufu, S. T. Staggs, O. Stryzak, C. Visnjic, K. W. Yoon, and Y. Zhao, "The Atacama B-Mode Search: CMB Polarimetry with Transition-Edge-Sensor Bolometers," *American Institute of Physics Conference Series* **1185**, 494–497 (2009).
  16. H. Tran, B. Johnson, M. Dragovan, J. Bock, A. Aljabri, A. Amblard, D. Bauman, M. Betoule, T. Chui, L. Colombo, A. Cooray, D. Crumb, P. Day, C. Dickenson, D. Dowell, S. Golwala, K. Gorski, S. Hanany, W. Holmes, K. Irwin, B. Keating, C.-L. Kuo, A. Lee, A. Lange, C. Lawrence, S. Meyer, N. Miller, H. Nguyen, E. Pierpaoli, N. Pontheiu, J.-L. Puget, J. Raab, P. Richards, C. Satter, M. Seiffert, M. Shi-

- mon, B. Williams, and J. Zmuidzinas, "Optical design of the EPIC-IM crossed Dragone telescope," Society of Photo-Optical Instrumentation Engineers (SPIE) Conference Series **7731**, 77311R (2010).
- 17. M. D. Niemack, P. A. R. Ade, J. Aguirre, F. Barrientos, J. A. Beall, J. R. Bond, J. Britton, H. M. Cho, S. Das, M. J. Devlin, S. Dicker, J. Dunkley, R. Dünner, J. W. Fowler, A. Hajian, M. Halpern, M. Hasselfield, G. C. Hilton, M. Hilton, J. Hubmayr, J. P. Hughes, L. Infante, K. D. Irwin, N. Jarosik, J. Klein, A. Kosowsky, T. A. Marriage, J. McMahon, F. Menanteau, K. Moodley, J. P. Nibarger, M. R. Nolta, L. A. Page, B. Partridge, E. D. Reese, J. Sievers, D. N. Spergel, S. T. Staggs, R. Thornton, C. Tucker, E. Wollack, and K. W. Yoon, "ACTPol: a polarization-sensitive receiver for the Atacama Cosmology Telescope," Society of Photo-Optical Instrumentation Engineers (SPIE) Conference Series **7741**, 77411S (2010).
  - 18. C. Granet, "Designing classical Dragonian offset dual-reflector antennas from combinations of prescribed geometric parameters," IEEE Antennas and Propagation Magazine **43**, 100–107 (2001).
  - 19. J. W. Fowler, M. D. Niemack, S. R. Dicker, A. M. Aboobaker, P. A. R. Ade, E. S. Battistelli, M. J. Devlin, R. P. Fisher, M. Halpern, P. C. Hargrave, A. D. Hincks, M. Kaul, J. Klein, J. M. Lau, M. Limon, T. A. Marriage, P. D. Mauskopf, L. Page, S. T. Staggs, D. S. Swetz, E. R. Switzer, R. J. Thornton, and C. E. Tucker, "Optical design of the Atacama Cosmology Telescope and the Millimeter Bolometric Array Camera," Applied Optics **46**, 3444–3454 (2007).
  - 20. S. Padin, Z. Staniszewski, R. Keisler, M. Joy, A. A. Stark, P. A. R. Ade, K. A. Aird, B. A. Benson, L. E. Bleem, J. E. Carlstrom, C. L. Chang, T. M. Crawford, A. T. Crites, M. A. Dobbs, N. W. Halverson, S. Heimsath, R. E. Hills, W. L. Holzapfel, C. Lawrie, A. T. Lee, E. M. Leitch, J. Leong, W. Lu, M. Lueker, J. J. McMahon, S. S. Meyer, J. J. Mohr, T. E. Montroy, T. Plagge, C. Pryke, J. E. Ruhl, K. K. Schaffer, E. Shirokoff, H. G. Spieler, and J. D. Vieira, "South Pole Telescope optics," Applied Optics **47**, 4418–4428 (2008).
  - 21. M. J. Griffin, J. J. Bock, and W. K. Gear, "Relative performance of filled and feedhorn-coupled focal-plane architectures," Applied Optics **41**, 6543–6554 (2002).
  - 22. R. Datta, J. Hubmayr, C. Munson, J. Austermann, J. Beall, D. Becker, H. M. Cho, N. Halverson, G. Hilton, K. Irwin, D. Li, J. McMahon, L. Newburgh, J. Nibarger, M. Niemack, B. Schmitt, H. Smith, S. Staggs, J. Van Lanen, and E. Wollack, "Horn Coupled Multichroic Polarimeters for the Atacama Cosmology Telescope Polarization Experiment," Journal of Low Temperature Physics **176**, 670–676 (2014).
  - 23. R. Datta, C. D. Munson, M. D. Niemack, J. J. McMahon, J. Britton, E. J. Wollack, J. Beall, M. J. Devlin, J. Fowler, P. Gallardo, J. Hubmayr, K. Irwin, L. Newburgh, J. P. Nibarger, L. Page, M. A. Quijada, B. L. Schmitt, S. T. Staggs, R. Thornton, and L. Zhang, "Large-aperture wide-bandwidth antireflection-coated silicon lenses for millimeter wavelengths," Applied Optics **52**, 8747 (2013).